

**GENERATING A CONSISTENT FRAMEWORK FOR EVALUATING CELL  
RESPONSE TO EXTERNAL STIMULI THROUGH EPIGENETIC ASSESSORS**

A Thesis

by

BO WANG

Submitted to the Office of Graduate Studies of  
Texas A&M University  
in partial fulfillment of the requirements for the degree of

MASTER OF SCIENCE

May 2011

Major Subject: Chemical Engineering

Generating a Consistent Framework for Evaluating Cell  
Response to External Stimuli through Epigenetic Assessors

Copyright 2011 Bo Wang

**GENERATING A CONSISTENT FRAMEWORK FOR EVALUATING CELL  
RESPONSE TO EXTERNAL STIMULI THROUGH EPIGENETIC ASSESSORS**

A Thesis

by

BO WANG

Submitted to the Office of Graduate Studies of  
Texas A&M University  
in partial fulfillment of the requirements for the degree of  
MASTER OF SCIENCE

Approved by:

Chair of Committee,	Mariah Hahn
Committee Members,	Arul Jayaraman
	Melissa Grunlan
Head of Department,	Michael Pishko

May 2011

Major Subject: Chemical Engineering

## **ABSTRACT**

Generating a Consistent Framework for Evaluating Cell Response to External Stimuli  
through Epigenetic Assessors. (May 2011)

Bo Wang, B.S., Tianjin University

Chair of Advisory Committee: Dr. Mariah Hahn

Mesenchymal stem cells are more and more widely used in tissue engineering due to their pluripotency and no relative ethical problems. Traditional characterization techniques to detect mesenchymal stem cell states include flow cytometry, gene expressing profiling and immunohistochemistry. However, these methods can only provide transient and low level information from current RNA or protein levels about mesenchymal stem cells, which may cause problems when predicting the possible downstream lineages they will commit into.

We have developed chromatin immunoprecipitation (ChIP)-based epigenetic technique to detect mesenchymal stem cell states. For the systems we tested, this epigenetic assessor successfully characterized cell state changes and gave similar results obtained from gene expression profiling or protein expression assay. This epigenetic technique can provide information about mesenchymal stem cells states from a more fundamental chromatin level, which is promising for predicting future lineages from current states.

## ACKNOWLEDGEMENTS

My advisor, Dr. Mariah Hahn, has been a phenomenal mentor to me. I've learned a lot from her. Her patience, advice and guidance have been invaluable. The direction she has given me has allowed me to grow and develop my capabilities as a qualified researcher. The enthusiasm for science she has imparted to me has made me enjoy my research very much.

I want to thank my committee members, Dr. Arul Jayaraman and Dr. Melissa Grunlan. They provided a lot of helpful insights and feedbacks. I'm especially grateful to Dr. Jayaraman for his permission to use the imaging system in his lab.

I want to thank all of the graduate students of the Hahn lab who have helped me during my time there and created a friendly and stimulating lab culture. Xin Qu, Dany Munoz-Pinto, Rebecca McMahon, Carolina Jimenez all welcomed me and taught me mammalian cell techniques. I also want to thank the younger students, Viviana Guiza and Silvia Becerra with whom I have enjoyed sharing reagents.

I also want to thank Dr. Thomas Wood, his student Qun Ma and post docs, Xiaoxue Wang and Mingming Pu, for their permission to do protein work in their lab and for their help.

I want to thank my parents for their love and support and encouraging me to devote myself to science.

Last but not least, I'd like to thank my wife, Ying. Without her, I could not have finished my research and my thesis.

## TABLE OF CONTENTS

	Page
ABSTRACT .....	iii
ACKNOWLEDGEMENTS .....	iv
TABLE OF CONTENTS .....	v
LIST OF FIGURES .....	vii
1. INTRODUCTION.....	1
1.1 Mesenchymal stem cells (MSC) in tissue engineering .....	1
1.2 Epigenetic assessors for detection of stem cell states .....	8
1.3 A widely used matrix in tissue engineering--PEGDA.....	12
2. EPIGENETIC STUDY OF MODEL SYSTEMS .....	13
2.1 Development of ChIP for 3D cell cultures.....	13
2.1.1 Summary .....	13
2.1.2 Materials and methods.....	13
2.1.3 Results .....	15
2.1.4 Discussion .....	17
2.2 Growth factor stimulated systems .....	18
2.2.1 Summary .....	18
2.2.2 Materials and methods.....	18
2.2.3 Results .....	19
2.2.3.1 TGFb treated C3H10T1/2 systems.....	19
2.2.3.2 Insulin treated 3T3-L1 systems .....	20
2.2.4 Discussion .....	22
2.3 PEGDA matrix systems.....	23
2.3.1 Summary .....	23
2.3.2 Materials and methods.....	23
2.3.3 Results .....	25
2.3.3.1 C3H/10T1/2 model system.....	25
2.3.3.2 NIH/3T3 model system.....	28
2.3.4 Discussion .....	30
3. CONCLUSIONS AND FUTURE DIRECTIONS .....	32
3.1 Conclusions.....	32
3.2 Future directions .....	33

	Page
3.2.1 Effects of matrices elasticity on stem cell differentiation .....	33
3.2.2 Epigenetic changes in 3D cell cultures.....	34
REFERENCES .....	36
VITA.....	41

## LIST OF FIGURES

	Page
Figure 1 Cell response is affected by a variety of input stimuli including: (1) soluble regulators; (2) external strain; (3) cell-cell interactions; (4) matrix properties (matrix- mediated stimuli); and (5) initial cell state .....	2
Figure 2 Chromatin landscape of a cellular gene whose expression is regulated by transcription factor SRF .....	5
Figure 3 3T3-L1, NIH/3T3 and C3H/10T1/2 cells are mouse mesodermal or mouse mesodermal-derived cells .....	6
Figure 4 Scheme of histone modification pathways.....	10
Figure 5 Scheme of Chromatin Immunoprecipitation (ChIP) .....	11
Figure 6 Fragmented C3H/10T1/2 cells chromatin by sonication .....	15
Figure 7 Fragmented C3H/10T1/2 cells chromatin by enzymatic digestion .....	16
Figure 8 SRF enrichment of different genes in C3H10T1/2 cells encapsulated in PEGDA matrices.....	17
Figure 9 Relative histone enrichment of different genes in C3H10T1/2 cells .....	20
Figure 10 Relative histone enrichment of different genes in 3T3-L1 cells.....	21
Figure 11 Relative RNA expression level of different genes in 3T3-L1 cells .....	21
Figure 12 Relative histone enrichment of different genes in C3H10T1/2 cells .....	26
Figure 13 Relative RNA expression level of different genes in C3H10T1/2 cells.....	26
Figure 14 Relative RNA expression level of cell markers in C3H10T1/2 cells .....	27
Figure 15 Relative protein expression levels in C3H10T1/2 cells .....	27
Figure 16 Relative histone enrichment of different genes in NIH/3T3 cells .....	28
Figure 17 Relative RNA expression level of different genes in NIH/3T3 cells .....	29
Figure 18 Relative RNA expression level of cell markers in NIH/3T3 cells.....	29
Figure 19 Relative protein expression level in NIH/3T3 cells .....	30



## 1. INTRODUCTION

### 1.1 Mesenchymal stem cells (MSC) in tissue engineering

Tissue loss or end-stage organ failure causes more and more severe problems all over the world. Every year, the total national health care cost for patients suffering these problems exceeds \$400 billion in US alone (1). As a traditional treatment, tissue transplantation saves a large number of patients (1). However, due to the donor shortage and increasing number of patients, people are looking for new curing methods. Since its foundation, tissue engineering (1, 2) has been used more and more. During the decade, FDA has approved the application of a larger number of artificial tissues in vivo (3).

Stem cells expose their great potential for application in tissue engineering (4) since they were discovered. Various kinds of stem cells have been investigated clinically (5, 6). Among these, mesenchymal stem cells (MSC) are most widely used as a result of their pluripotency and none ethical problems associated. They are able to differentiate into osteoblasts, chondrocytes, adipocytes and myocytes under corresponding stimuli. Our lab has a long history of studying mouse mesenchymal stem cells. We have successfully investigated the effects of pore size and modulus of matrices on their differentiation in 3D cultures (7, 8).

MSC behavior at a given time point is the output result of a multitude of input stimuli (**Figure 1**), each of which influences cell gene expression through modulation of internal signaling pathways. These stimuli act individually and in concert to direct MSC lineage progression. Soluble factors, such as TGF- $\beta$  and dexamethasone, are currently the most widely used means of directing MSC differentiation. However, MSC responses to soluble signals can be profoundly influenced by the concomitant, matrix-mediated signals the cells receive. For instance, the osteogenic tendency of MSCs cultured in the

---

This thesis follows the style of *Proceedings of the National Academy of Science of the United States of America*.

presence of dexamethasone and ascorbic acid on collagen type I-coated tissue culture polystyrene (TCPS) is effectively negated on fibronectin-coated TCPS (9).

Despite these advances, our understanding of cell behavior is not yet sufficient to enable the rational selection of stimuli to elicit desired cell responses. Indeed, the literature contains a number of recent examples of the same apparent stimuli being

applied to MSCs with markedly different outcomes. For instance, a recent study found that MSCs cultured in alginate gels in the presence of TGF- $\beta$  and dexamethasone displayed decreased chondrogenic potential with increasing levels of integrin-adhesion peptide RGD (12). In contrast, a separate study reported that MSCs cultured in PEG-based hydrogels, also in the presence of TGF- $\beta$  and dexamethasone, showed increased chondrogenic potential with increasing RGD concentration (13). Since neither PEG nor alginate interacts significantly with cells and since neither study characterized gel modulus, the source of the discrepancy between the two studies is, as is often the case, unclear. Such inconsistencies limit our ability to rationally guide MSC lineage progression.

A fundamental premise is that many of these apparently conflicting results are actually consistent, but appear to be in disagreement due to the need for further specification and/or control of the context in which cell stimulation is occurring. Three primary contextual factors include: 1. the complexity of microenvironments normally used to study matrix-mediated signaling (this complexity frequently confounds questions of relative stimuli impact); 2. differences in the initial cell population “state” not accounted for by conventional cell marker assessments; 3. differences in the stage of temporal evolution at which the system is examined.

Moreover, as the most widely used technique to characterize cells states in artificial tissues, immunohistochemistry can not give the quantitative state of cells due to its qualitative property. Unspecific background binding of antibodies can also happen all the time, which will result in inexact conclusions. In this case, a new detection technology is needed to characterize cell states in artificial tissues to help identifying the function of them more exactly.

The overall goal of this work is to develop a ChIP (chromatin immunoprecipitation)-based epigenetic method to characterize differential states of stem

cells in artificial tissues.

An additional key challenge to the development of cause-effect relationships arises from the limited characterization of initial “cell state” incorporated in most tissue engineering studies. Current MSC characterization methods serve as an excellent example of this. The pluripotent character of MSCs is, at present, generally assessed by flow cytometry analyses of a set of cell markers (CD105<sup>+</sup>, CD44<sup>+</sup>, CD166<sup>+</sup>, CD29<sup>+</sup>, CD14<sup>-</sup>, CD34<sup>-</sup>, CD45<sup>-</sup>). Despite the continued expansion of this cell marker set, dramatic variations in the differentiation potential of “confirmed” MSCs (i.e. MSCs with quantitatively similar cell marker profiles) are documented (14). Importantly, not all of these behavioral differences can be attributed to genetics. Thus, there are critical aspects of MSC pluripotency which are not being captured by these conventional cell marker analyses. Similar comments apply to primary differentiated cells. Thus, improved methods for characterizing “cell state” are needed to enable discovery of causative relationships between applied input stimuli and observed cell responses.

But what are these “improved”/“adequate” assessors? Gene expression data alone are insufficient, because the gene expression analyses provide only a momentary snapshot of the cell while giving limited insight into the direction in which the cell is headed. Transcription factor profiles can give deeper insight into future paths of cell response, but are also not adequate. This is because transcription takes place on promoter DNA within the context of chromatin and that the structure of this chromatin plays an active and fundamental role in transcriptional control. To see this, we can examine the two distinct histone landscapes, shown schematically in **Figure 2** for a gene expressed in response to binding of transcription factor SRF. Even if the cell is expressing abundant SRF, the expression of SRF-induced genes will be low if the gene histone-coding pattern is of a heterochromatic format. Thus, our hypothesis is that some level of the cell

population-average, epigenetic landscape must be characterized, in conjunction with transcription factors profiles, to adequately specify “cell state”. To test this hypothesis, we will exploit differences in the differentiation potentials of three mouse embryonic mesodermal-derived cell lines: C3H/10T1/2, NIH/3T3 and 3T3-L1. We have chosen to use these pluripotent cell lines instead of human MSCs, since these mouse cell lines retain the pluripotency characteristic of human MSCs while giving more highly reproducible responses with population doubling. This consistency in initial “cell state” with general cell expansion is required for the rapid screening of chromatin-based assessors indicative of alterations in cell responses induced by an applied stimulus. Although the use of mouse cells does mean that our work will be less immediately applicable to the human system, the results will establish a framework which can one day be expanding to understanding human MSCs.

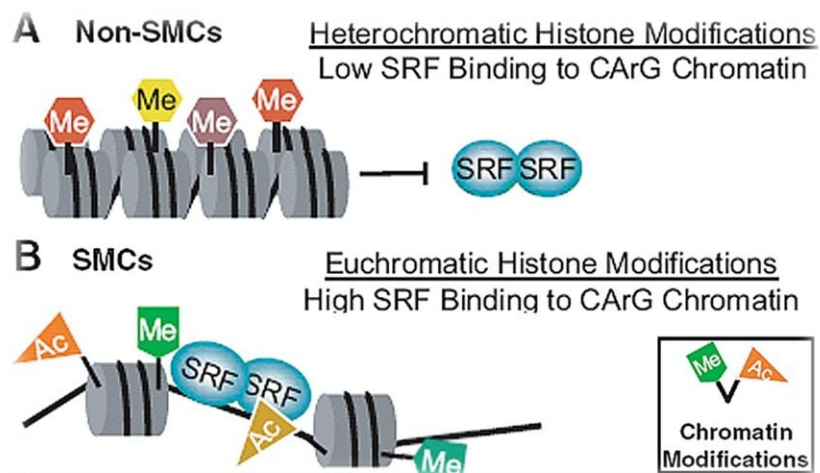


**Figure 2 Chromatin landscape of a cellular gene whose expression is regulated by transcription factor SRF**

The distinctions in the differentiation tendencies among the three selected model cell

lines are broadly depicted in **Figure 3**. Specifically, 10T1/2 cells have a tendency to progress toward muscle-like fates, while the random fate decisions of NIH/3T3 cells appear to be more evenly distributed among potential lineages. It is our premise that these consistent differences in tendency reflect differences in initial “cell state” (epigenetic landscape) among the cell lines. However, restricting our observations to 10T1/2 and NIH/3T3 cells would not allow us to rule out genetic effects as a primary source of observed differences. Therefore, we will also examine the stimuli responses of 3T3-L1 cells, a line directly derived from and genetically identical to NIH/3T3 cells but with significantly altered differentiation tendencies.

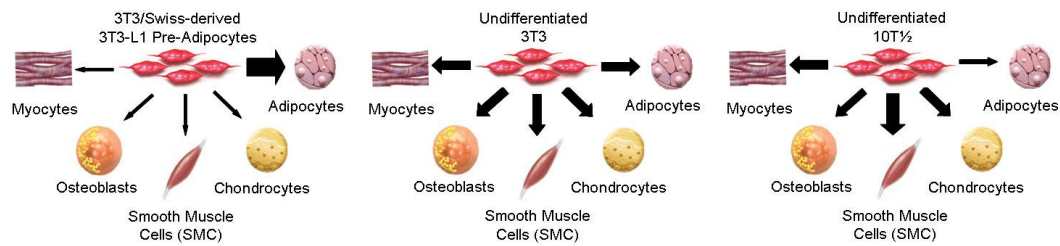


**Figure 3 3T3-L1, NIH/3T3 and C3H/10T1/2 cells are mouse mesodermal or mouse mesodermal-derived cells**

In executing the proposed studies, we will expose each of the three cell lines to the same stimulus combinations and screen for alterations associated with the induced population fate decisions via two methods: 1. comparison of alterations in the protein-level profiles of standard cell markers associated with retention of pluripotency as well as a subset of transcription factors associated with lineage specific differentiation (**Table 1**); 2. comparison of alterations in the histone profiles of genes associated with pluripotency and genes encoding for transcription factors associated with lineage specific differentiation. For approach 2, a limited subset of histone modifications (3-4

different modifications) will be examined per screening cycle, with 2 examples of common histone modifications given in **Table 1**. By combining these various assessors of alterations in population average “cell state” induced by the application of a specific stimulus with systems biology approaches, we will identify histone-code “signatures” which are highly correlated with observed population average, cell-fate trajectories. While these initial associations will be inherently correlative, the establishment of these initial correlative links will enable later assessment of causative links.

Futhermore, the model systems we choose are all valid model systems as all of the three kinds of cells are used a lot in tissue engineering (15, 16, 17). Combining the changes in all three stages of DNA (histone modifications), RNA and protein can give us an integrative overview of cell states, which is more complete than the information that can be obtained through immunohistochemistry. Moreover, the study of these model systems can provide more promise for application of this method in other cell systems, or even in the whole tissue engineering.

**Table 1 Example of genes and histones to be examined**

<b>Standard Genes associated with Specific Cell Population Lineage Progression</b>	<b>Two Examples of Common Histone Modifications</b>
<b>Multipotent:</b> CD105 <b>Osteogenic:</b> Runx2 <b>Chondrogenic:</b> Sox9 <b>Smooth Muscle:</b> Myocardin <b>Myogenic:</b> MyoD <b>Adipogenic:</b> PPAR $\gamma$	<b>H4Ac:</b> generally associated with euchromatin <b>H3K27Me3:</b> generally associated with heterochromatin

## **1.2 Epigenetic assessors for detection of stem cell states**

To our knowledge, this is the first time that epigenetic study has undergone in tissue engineering. Epigenetics has been studied for a long time (18), and recently, more and more physiological phenomena have been related with epigenetic reprogramming in vivo (19). Moreover, a lot of work has been done on the characterization of the epigenetic states of stem cells (20). However, little work has been done on the identification of epigenetic states during differentiation process of stem cells, especially for those encapsulated in artificial tissues. Our work provides ways to investigate these basic chromatin dynamics to better understand the mechanisms of stem cells differentiation, to direct their differentiation more effectively and to predict their differentiation from DNA stage, a much deeper perspective than from protein stage, which is normally revealed by immunohistochemistry.

Stem cells play a very important role in tissue engineering (4). Once they are encapsulated in artificial matrices, they can be directed to differentiate into various kinds of cells depending on the small moieties in the matrices (21), or the elasticity of matrices (10, 22). On the other hand, different growth factors or motifs can be cross-linked in the matrices either physically or chemically to guide differentiation more specifically and efficiently (23, 24).

Stem cells are also well characterized in their epigenetic states (20), expression profiles (25) and pluripotency (26). Epigenetic study usually consists of two different aspects: methylation in DNA CpG islands (27) and histone modifications in chromatin (28).

DNA methylation involves the addition of a methyl group to the 5 position of the cytosine pyrimidine ring, which may be essential for normal development and is associated with a number of key processes including genomic imprinting, X-chromosome inactivation, suppression of repetitive elements and carcinogenesis.



There are large numbers of repeating sequences in mammalian cells, which are full of CpG dinucleotides. Once methylated, transcription factors may not be able to bind to the gene, which will lead transcriptional silencing. The most common technique used to characterize DNA methylation is bisulfite sequencing. Treatment of DNA with bisulfite converts cytosine residues to uracil, but leaves 5-methylcytosine residues unaffected. Then specific primers are used to sequence the fragment, providing single nucleotide resolution information about the methylated sites. So a sequencer is needed to detect methylation in DNA. Due to the limit of instruments, at this stage, our work will focus on histone modifications in chromatin, which is characterized very well in stem cells (20).

Chromatins are composed of DNA and histones, both of which are dynamic in vivo. Histones are composed of four core subunits H2A, H2B, H3 and H4 and two linker units H1 and H5. Two of each of the four core histones form an octameric assembly and 147 bp of DNA winds the assembly to form a nucleosome. Histone modifications include methylation, acetylation and phosphorylation of specific amino acid residues. **Figure 4** shows the scheme of histone modification pathways (29). Among these four core histones, modifications usually occur on lysine, serine and arginine residues in H3 and H4 (29, 30, 31, 32, 33) (**Figure 4**). Different histone modifications will cause chromatin to alter between euchromatin, which is a lightly packed form of chromatin and under active transcription, and heterochromatin, which is a tightly packed form of chromatin and under gene silencing.

Among all of these modifications, methylation at H3K4, H3K9, H3K27, H3K36 and H3K79 and acetylation at H3K9/14 are of most importance. H3K9/14Ac usually results in a euchromatin state for active transcription of genes. However, different levels of methylation correspond to different chromatin states (29, 31, 32). For example, H3K4 tri-methylation is associated with transcription activation and usually occurs near the

transcription start sites of actively transcribed genes (20, 31).

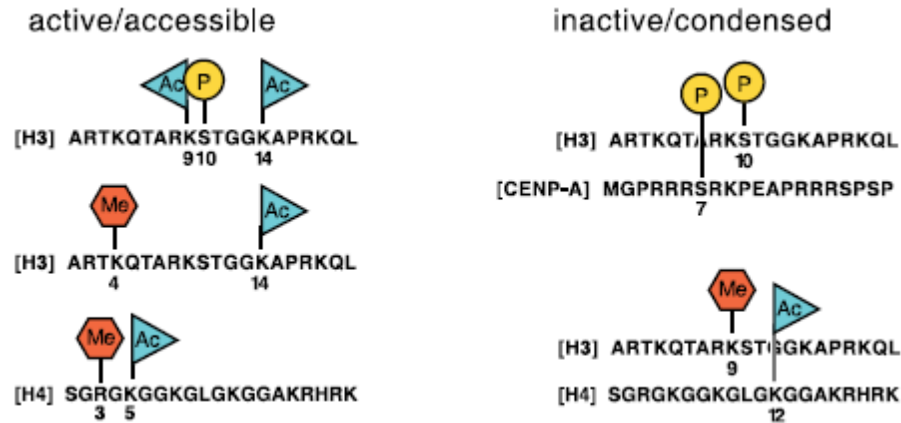


**Figure 4** Scheme of histone modification pathways

H3K9 tri-methylation and H3K27 tri-methylation are associated with transcription repression (31), but H3K9 mono-methylation and H3K27 mono-methylation are associated with transcription activation. H3K36 tri-methylation and H3K79 di-methylation are associated with transcription elongation and occur within the body of transcriptionally active gene (20). In this work, we focus on H3K4 tri-methylation, H3K9 tri-methylation, H3K27 tri-methylation and H3K9/14 acetylation.

Originally used as a technique to detect DNA-protein interactions, ChIP (chromatin immunoprecipitation) plays more and more important role in epigenetic study (34). The scheme of ChIP is shown in **Figure 5**. After fragmentation of DNA, specific antibodies are used to immunoprecipitate different proteins bound to DNA. Then DNA/protein/antibody complex is reversecross-linked, and the eluted DNA will be used for PCR, qPCR, direct sequencing, or microarray (35).

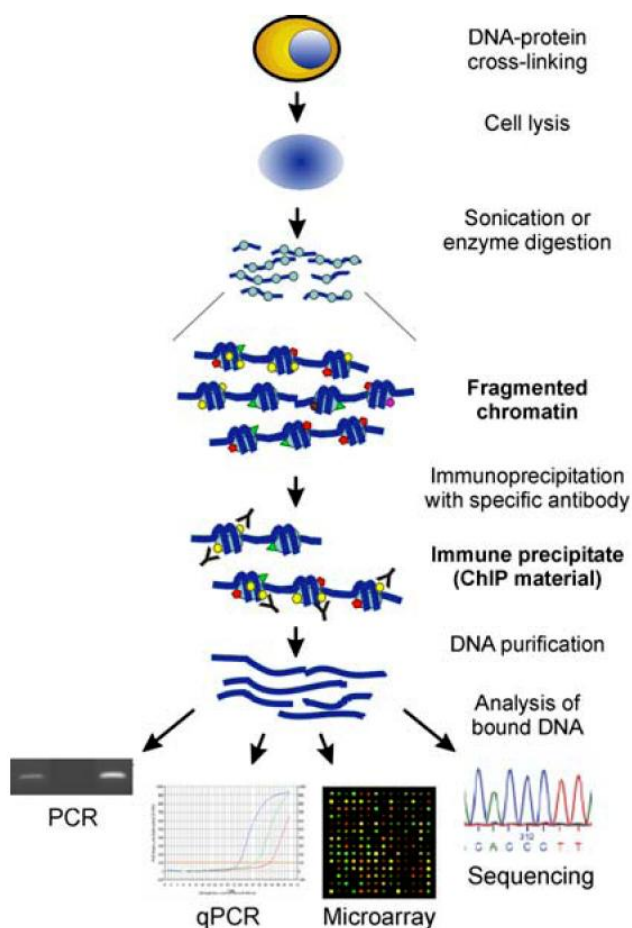


**Figure 5 Scheme of Chromatin Immunoprecipitation (ChIP)**

RNA profiling is a commonly used technique to obtain information about different genes' expression levels. In our system, one-step qRT-PCR is used. Trizol extracted RNA is first reverse transcribed into cDNA by gene specific primers, then these primers are used to amplify cDNA exponentially to measure its level, which is indicative of original RNA level. Different RNA expression levels are usually caused by different states of cells, or more basically, different responses of cell to environment stimuli.

ELISA (enzyme-linked immunosorbent assay) is a widely used method to check the levels of target antigen in samples. Primary antibody binds to antigen first, and

enzyme-conjugated secondary antibody binds to primary antibody, which will cause the enzymatic color change of reactive substrate. Then through the extent of color change in the system, we can know the levels of target antigen in samples sensitively and easily.

### **1.3 A widely used matrix in tissue engineering--PEGDA**

In this work, we will use PEG-based artificial matrices. PEG has many advantages for application in tissue engineering: 1. PEG is biocompatible, hydrophilic polymer, which can be used safely with cells and does not adsorb proteins (actually, it's approved for in vivo use by FDA); 2. PEG has a well-established chemistry, which can form photo cross-linked network after acrylation; 3. matrices elasticity can be easily modulated through using of different molecular weight macromers (36). For these reasons, PEG is widely used in tissue engineering. Recently, the application of matrix metalloproteinase target peptide sequence (GPQGIWGQK) (12) imparts the ability of cell-based degradation to PEG matrices. Along with the pegylation of different growth factors to induce cell differentiation or tissue regeneration, a more advanced cell degradable, tissue regenerative matrix has been made to simulate in vivo extracellular environment more effectively (23).

## **2. EPIGENETIC STUDY OF MODEL SYSTEMS**

### **2.1 Development of ChIP for 3D cell cultures**

#### **2.1.1 Summary**

Before we investigate our model systems, we need to optimize experiment conditions to give reliable results. The most important step in ChIP is chromatin fragmentation. Over-fragmentation may diminish signal in the qPCR quantification, and under-fragmentation may cause increasing background signal and lower resolution. So our aim is to fragment chromatin to 150-450bp. In order to obtain the optimized chromatin fragments, namely, 150 to 450bp, we have tried 2 methods, sonication and enzymatic digestion. After that, we tested ChIP in 3D cell cultures.

#### **2.1.2 Materials and methods**

Fragmentation of chromatic DNA by sonication is done as following. Add 1% final concentration of formaldehyde (Sigma-Aldrich) to  $2 \times 10^6$  C3H/10T1/2 cells to cross-link proteins to DNA at room temperature (RT) for 10min with gentle shaking. Then add 125mM final concentration of glycine (Fisher Scientific) to quench the formaldehyde with gentle shaking for 5min at RT. After that, rinse cells twice with 8ml ice-cold PBS (Sigma-Aldrich). Then scrape cells into 4ml PBS+PMSF (Sigma-Aldrich) (1mM final concentration), centrifuge at 1500rpm at 4°C for 5min. After that, resuspend cells in 500ul ChIP buffer (Santa Cruz Biotechnology). Then cells are sonicated at different conditions to fragment chromatin. Fragmented chromatin is used in reverse cross-linking to analyze DNA fragmentation.

Enzymatic fragmentation of chromatic DNA is done as following. Add 1% final concentration of formaldehyde to  $2 \times 10^6$  C3H/10T1/2 cells to cross-link proteins to DNA at room temperature (RT) for 10min with gentle shaking. Then add 125mM final concentration of glycine to quench the formaldehyde with gentle shaking for 5min at RT. After that, rinse cells twice with 8ml ice-cold PBS. Then scrape cells into 4ml

PBS+PMSF (1mM final concentration), centrifuge at 1500rpm at 4°C for 5min. After that, resuspend cells in 500ul Buffer A+DTT+PIC+PMSF (Cell Signaling Technology) and incubate on ice for 10min with inverting tube every 3min. Then centrifuge at 3000rpm for 5min at 4°C, resuspend pellet in 500ul Buffer B+DTT (Cell Signaling Technology). Repeat centrifugation, resuspend pellet in 50ul Buffer B+DTT. Add 1-5ul micrococcal nuclease (New England Biolabs) to digest chromatin at 37°C for 20min by inverting tube every 3min. Then stop digest by 100ul 0.5M EDTA (Cell Signaling Technology), centrifuge at 13000rpm for 1min at 4°C, resuspend pellet in 500ul ChIP buffer+PIC+PMSF (Cell Signaling Technology), incubate on ice for 10min. Then pellets are sonicated to break nuclear membrane. Centrifuge at 10000rpm for 10min at 4°C, supernatant is used in reverse cross-linking to analyze DNA fragmentation.

ChIP for C3H10T1/2 cells in PEGDA hydrogels is done as following. The same procedure is used to collect chromatin, except homogenizing hydrogels with microbeads to release cells, then using 0.12N NaOH to digest hydrogel particles for 24hrs after using glycine to quench formaldehyde. After that, 7.5ug specific antibodies (Santa Cruz Biotechnology) targeting different proteins are added to 100ul cross-linked chromatin+400ul ChIP buffer and incubated at 4°C overnight (o/n) with rotation. Then add 30ul protein G agarose beads (Cell Signaling Technology) and incubate at 4°C for 2hrs with rotation. Then beads are washed sequentially with low salt wash buffer (Cell Signaling Technology) and high salt wash buffer (Cell Signaling Technology). After that, they are reversed cross-linked at 65°C for 2hrs to elute DNA. QIAquick PCR Purification Kits (Qiagen) are used to purify eluted DNA.

Real-time PCR is done as following. Real-time PCR are run in ABI7500 system (Applied Biosystems) with gene specific primers (SABiosciences), using ABI master mix (Applied Biosystems).

### 2.1.3 Results

The effect of chromatin fragmentation by sonication is shown. Initially, we used sonication to fragment chromatin. **Figure 6** shows the results of chromatin fragmentation under different sonication conditions. We tried different output powers and different number of cycles. Each cycle was composed of 10s sonication on ice and 10s pause on ice. We can see that although sonication time and intensity are increased, chromatin is still not fragmented very well. A large proportion of chromatin is still above 1kb, which means even the highest intensity and longest time are not enough for the fragmentation level we need.

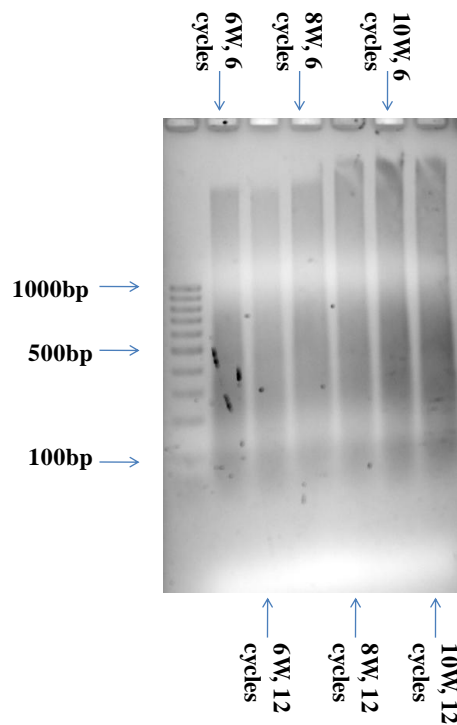


**Figure 6** Fragmented C3H/10T1/2 cells chromatin by sonication

The effect of chromatin fragmentation by enzymatic digestion is shown. Due to the power limit of the sonicator, we can not use higher intensity. So we changed to enzymatic digestion. Micrococcal nuclease is able to induce double-strand breaks within nucleosome linker regions, but only single-strand nicks within the nucleosome itself. So it can be used to digest chromatin. **Figure 7** shows the results of chromatin fragmentation using micrococcal nuclease. We can see that most chromatin is digested to the length of 1-3 nucleosomes. So we decided to use micrococcal nuclease to fragment chromatin in model systems.

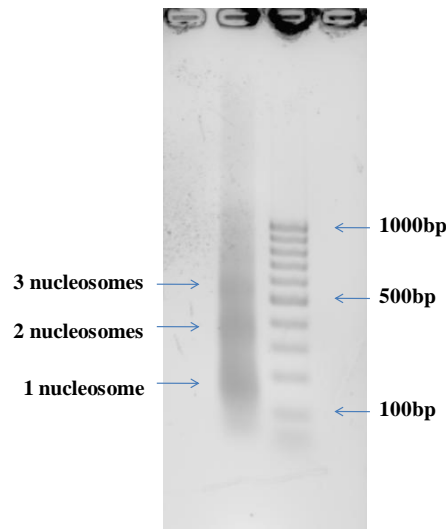


**Figure 7 Fragmented C3H/10T1/2 cells chromatin by enzymatic digestion**

The result of ChIP for C3H10T1/2 cells in PEGDA hydrogels is shown. Next, we conducted ChIP in 3D cultures. C3H10T1/2 cells were encapsulated in 6k PEGDA hydrogel with  $7.5 \times 10^6$  cells/ml PEG. After culturing in DMEM+10% d-FBS for 7days,



ChIP was performed with rat-anti-mouse SRF antibody. We found that after culturing in hydrogel for 7 days, about 1/240 of all SM-22a genes were bound by SRF, and about 1/4 of all c-fos genes were bound by SRF (**Figure 8**).

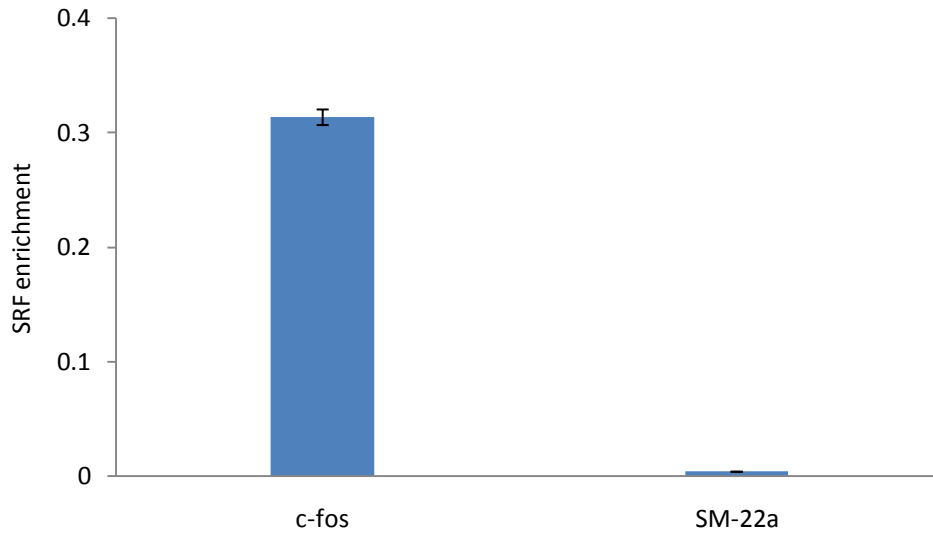


**Figure 8 SRF enrichment of different genes in C3H10T1/2 cells encapsulated in PEGDA matrices**

#### 2.1.4 Discussion

From the above results, we can see that for our system, enzymatic digestion is better than sonication for chromatin fragmentation. This may be due to more control of enzymatic digestion. Moreover, for histone modification-based ChIP, we need to fragmentate chromatin to 150-450bp. But sonication is much weaker.

On the other hand, NaOH digestion followed by enzymatic digestion can be used to collect chromatin. We hypothesize that NaOH can digest hydrogel particles left after homogenization, which will help to release cells still trapped. The digestion time is very

important for over-digestion may cause the degradation of DNA.

Moreover, SRF binding of SM-22a gene in C3H10T1/2 cells encapsulated in PEGDA hydrogels is important for their commitment into smooth muscle cells (SMC).

However, for ChIP in 3D cultures, a large number of punches (8) of hydrogels encapsulating cells are needed to collect enough chromatin, which is prohibitively high for sample demand compared to immunohistochemistry or RNA extraction (only need 2 or 3 punches). Due to the limit of amount of samples, we decide to transit to 2D study, which is easier to get large amount of chromatin.

## **2.2 Growth factor stimulated systems**

### **2.2.1 Summary**

Growth factors are widely used to stimulate differentiation of mesenchymal stem cells. Through recognizing their corresponding receptors on the cell membrane, activating their specific signaling pathways, they are able to induce cell states changes. Here, we use TGF- $\beta$  to stimulate C3H10T1/2 differentiation, and check modified histone binding to c-fos gene transcription start site, which is responsible for cell proliferation and to SM-22a gene transcription start site, which is a marker of differentiated smooth muscle cells (37). Next we use insulin to stimulate 3T3-L1 differentiation. 3T3-L1 cells have a very different differentiation potential compared to C3H10T1/2 cells. We will stimulate differentiation of 3T3-L1 cells (38), and compare cell states after stimulation to before stimulation from chromatin state and RNA expression level.

### **2.2.2 Materials and methods**

C3H/10T1/2 differentiation is done as following. C3H/10T1/2 cells at passage 10 are stimulated with DMEM (Invitrogen) +10% d-FBS (Thermo Scientific) supplemented with 1  $\mu$ g/ml ascorbic acid (Sigma-Aldrich), 1 ng/ml TGF- $\beta$  (Sigma-Aldrich). Media is changed every two days until day 7.

Other materials and methods are the same as in **2.1.2**, except the antibodies used:

Histone H3 (tri methyl K4) antibody (Abcam), Histone H3 (tri methyl K27) antibody (Abcam).

3T3-L1 differentiation is done as following. 2 days post-confluence, 3T3-L1 cells are induced to differentiate with DMEM +10%FBS supplemented with  $1\mu\text{M}$  dexamethasone (Sigma-Aldrich),  $0.5\text{mM}$  isobutylmethylxanthine (Sigma-Aldrich) and  $1\mu\text{g/ml}$  insulin (Sigma-Aldrich). After 2 days, the media is replaced with DMEM+10% FBS supplemented with  $1\mu\text{g/ml}$  insulin. After 2 days, cells are fed every 48h with DMEM+10%FBS for 4 days.

Other materials and methods are the same as in **2.1.2** and **2.3.2**.

### **2.2.3 Results**

#### **2.2.3.1 TGFb treated C3H10T1/2 systems**

**Figure 9** shows relative enrichment of transcription start sites of c-fos, SM-22a and RPL30 genes in C3H10T1/2 cells after treated with TGF-b compared to enrichment in their original culture. We can see that H3K4me3 enrichment of SM-22a gene is statistically significantly greater than H3K27me3 enrichment of the same gene, which predicts that SM-22a gene is actively transcribed. On the other hand, H3K4me3 enrichment of RPL30 gene is also greater than H3K27me3 enrichment of the same gene, which is a negative control. Even so, compared to times of which H3K4me3 enrichment of SM-22a is higher than H3K27me3 enrichment, we can still qualitatively find that SM-22a gene is actively transcribed. Due to the high standard deviation of H3K4me3 enrichment of c-fos gene, we are not able to get any conclusion about this gene.

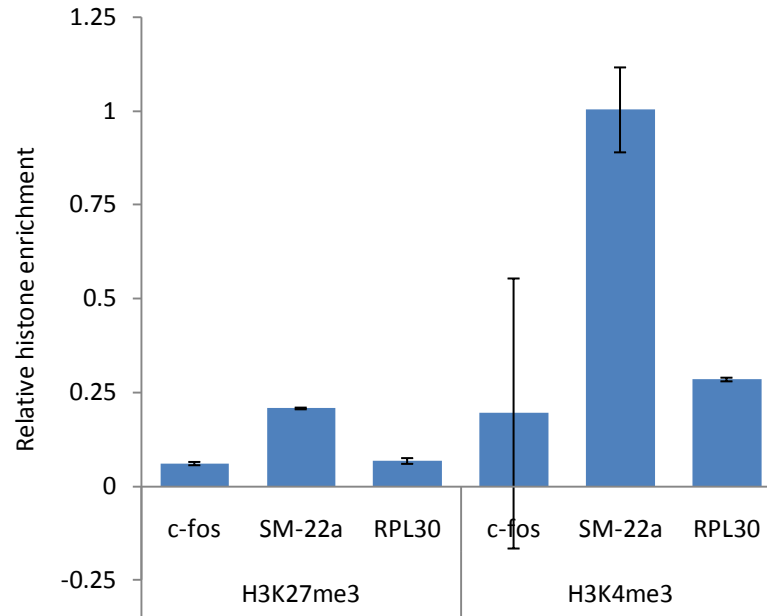


**Figure 9** Relative histone enrichment of different genes in C3H10T1/2 cells

### 2.2.3.2 Insulin treated 3T3-L1 systems

**Figure 10** shows relative enrichment of transcription start site of different genes in 3T3-L1 cells after stimulation compared to enrichment in their original culture. We can see that H3K4me3 enrichment of transcription start site of Pparg is statistically elevated compared to H3K27me3 and H3K9me3 enrichment of the same gene, which predicts the increased expression level of Pparg RNA. The statistically different enrichment of IGX1A by differently modified histones, which is a negative control, indicates that there are different backgrounds in each immunoprecipitation. Again, this can only allow us to qualitatively predict that Pparg gene will have increased expression level. Increased expression level of Pparg RNA in **Figure 11** supports the result. Moreover, the expression level of A-FABP RNA is also increased, which corresponds to the increased expression level of Pparg.

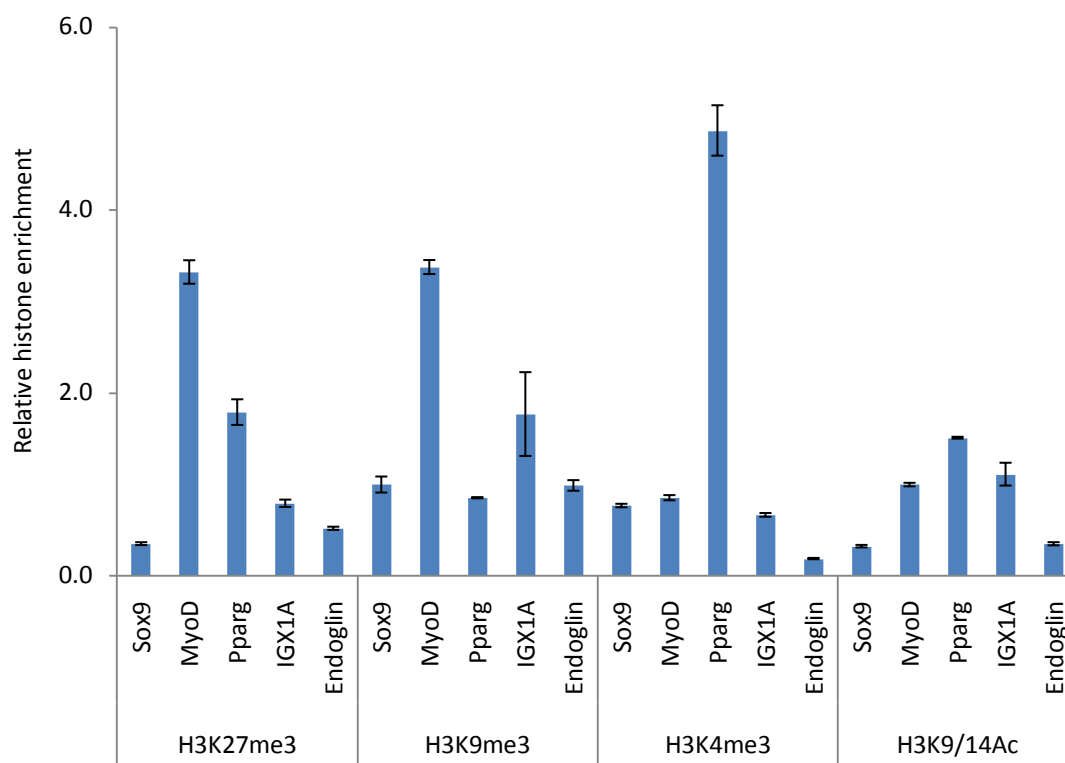


**Figure 10** Relative histone enrichment of different genes in 3T3-L1 cells

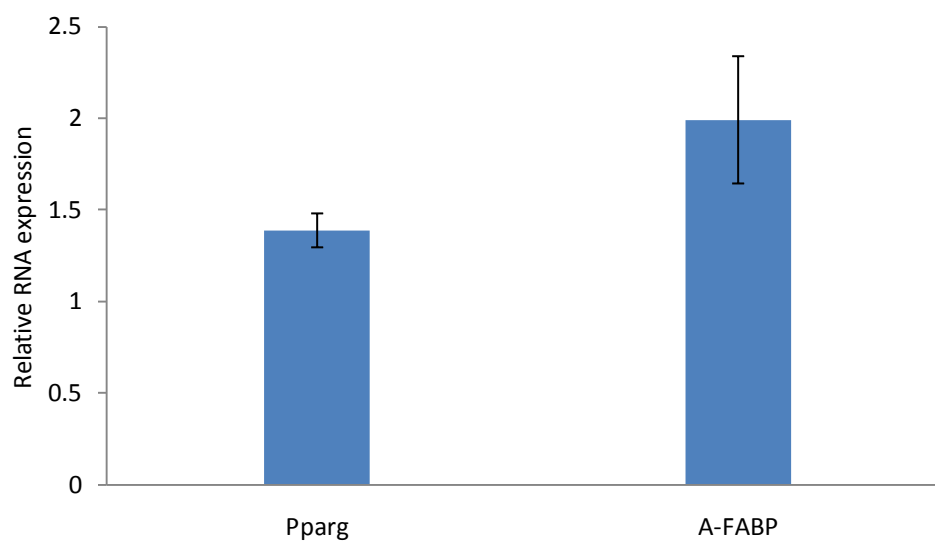


**Figure 11** Relative RNA expression level of different genes in 3T3-L1 cells

#### 2.2.4 Discussion

From the results above, due to the differences in enrichment levels of negative controls (RPL30 and IGX1A) by different modified histones in each system and the high standard deviations in enrichment levels of some genes such as c-fos, we are not able to get any statistically significant conclusions. But qualitatively, we can see that TGF- $\beta$  treated C3H/10T1/2 cells have more potential to become smooth muscle cells, and insulin treated 3T3-L1 cells have more potential to become adipocytes.

H3K4me3 enrichment of SM-22a gene promises elevated SM-22a RNA expression level, which in turn predicts increased SM-22a protein level. H3K4me3 enrichment of transcription start site of Pparg is increased, and Pparg and A-FABP RNA expression levels are also increased.

However, smooth muscle cells are only one lineage that C3H/10T1/2 cells can commit. It's possible that they differentiate into other lineages. And this study is limited to C3H/10T1/2 mesenchymal stem cells only. Moreover, growth factors stimulation is not commonly used in tissue engineering to regenerate tissues, which is prohibitively expensive. On the other hand, SM-22a is only a smooth muscle cell marker regulated by transcription factor SRF. If we can detect differently modified histone binding to transcription factors specific in a cell lineage, we are able to predict cell states from a deeper level.

So we propose to study epigenetic changes of C3H/10T1/2 cells seeded on PEGDA matrices surface. PEG is a kind of widely used hydrogel, so this work will provide more meaningful perspective to apply epigenetic techniques in tissue engineering. Moreover, we will check more kinds of modified histone binding to transcription start sites of multiple transcription factors. This will provide a wider viewpoint of cell states.

## **2.3 PEGDA matrix systems**

### **2.3.1 Summary**

Extracellular matrix (ECM) has very important effects on cell behaviors. In tissue engineering, it plays a even more important role for that it will determine viability of cells encapsulated in various scaffolds, responses of cells such as proliferation or differentiation (39). Actually, it is already verified that matrix with different modulus will cause human mesenchymal stem cells to commit into different lineages (10). For example, polyacrylamide matrix with small modulus will be neurogenic, while matrix with large modulus will be osteogenic. It is also verified that different moieties will cause human mesenchymal stem cells to commit into different lineages (21). For example, charged phosphate groups will be osteogenic, while hydrophobic t-butyl groups will be adipogenic. Based on these, we will study epigenetic changes in mouse mesenchymal stem cells seeded on PEG hydrogels. Mouse mesenchymal stem cells are similar to human mesenchymal stem cells, which are also pluripotent to differentiate various lineages and PEG hydrogels are similar to polyacrylamide, both of whose modulus can be adjusted by changing extent of cross-linking and macromers used. We will detect adipogenesis, chondrogenesis, and myogenesis of C3H/10T1/2 cells and NIH/3T3 cells using ChIP, then check the results from RNA and protein expression levels.

### **2.3.2 Materials and methods**

Cell seeding and culturing is done as following. C3H10T1/2 cells at passage 15 and NIH/3T3 cells at passage 11 are seeded at  $10^4$  cells/cm<sup>2</sup>. Before seeding, cells are treated with 8ug/ml mitomycin C (Sigma-Aldrich) for 4hrs to inhibit proliferation. After that, cells are trypsinized, collected and seeded on RGDS (American Peptide Company) tailored 20K 10% PEGDA (Sigma-Aldrich) hydrogel surfaces. Media is changed every two days until day 7.

RNA extraction is done as following. Enough Trizol (Invitrogen) is used to homogenize cells for 5min at RT. After homogenization, add corresponding amount of chloroform (Sigma-Aldrich), shake rigorously and centrifuge at 10000rpm at 4°C for 15min. After centrifugation, carefully transfer inorganic supernatant to a new tube, add equal volume of 70% ethanol (Sigma-Aldrich), mix thoroughly, then add solution to RNeasy columns (Qiagen) and centrifuge at 13000rpm for 30s. Repeat centrifugation until all the solution is added to the columns. Wash with Buffer RLP and RPE. Finally, elute RNA in 60ul nuclease-free water (Invitrogen).

Protein dialysis is done as following. Add corresponding amount of 100% ethanol (Sigma-Aldrich) to organic leftover after RNA extraction and centrifuge at 2000g at 4°C for 10min to get rid of rest DNA. Then put supernatant in 3500 MWCO (Thermo Scientific) dialysis membrane and dialyze against 0.1% SDS (Sigma-Aldrich) for 3 days or until the supernatant is colorless. After dialysis, centrifuge at 10000rpm at 4°C for 10min, discard the supernatant and dissolve the pellet in 200ul cell lysis buffer (0.1% SDS, 0.5% Triton X-100 (Sigma-Aldrich) in PBS).

RT-PCR is done as following. Real-time RT-PCR are run in one step in ABI7500 system with gene specific primers, using SuperScript III reverse transcriptase and Platinum<sup>®</sup> *Taq* DNA Polymerase mixture and 2X SYBR Green buffer (Invitrogen).

ELISA is done as following. Competitive blocking peptide (Santa Cruz Biotechnology) specific to target antigen (different cell lineage specific protein) is coated in a high-binding transparent plate o/n at 4°C. Next day, competitive ELISA is run. Briefly, samples are incubated with diluted 1<sup>o</sup> antibody at RT for 1hr, and at the same time the plate is blocked with 3% BSA in PBST. After this, samples are added to the plate in duplicate and incubated at RT for 1hr. Then diluted 2<sup>o</sup> antibody is added and incubated at RT for 45min. Finally, substrate ABTS (2, 2'-Azinobis [3-ethylbenzothiazoline-6-sulfonic acid]-diammonium salt) (Sigma) is added to the plate,



which will become a green product upon reaction with HRP, which is conjugated to 2° antibody.

Other materials and methods are the same as in 2.1.2.

### **2.3.3 Results**

We compared the states of C3H10T1/2 cells and NIH/3T3 cells in their original culture, where they are supposed to proliferate, to the states when attached to PEG-based matrices surfaces, where they are supposed to differentiate into different cell lineages based on matrices elasticity. In each case, we collected chromatin, RNA and protein samples separately for different analysis. Here, RGDS is used as cell binding motif (40).

#### **2.3.3.1 C3H/10T1/2 model system**

**Figure 12** shows relative enrichment of transcription start sites of different genes in C3H10T1/2 cells seeded on PEGDA surfaces compared to enrichment in their original culture. We can see that H3K4me3 enrichment of MyoD is greater than 1, which means MyoD gene is actively transcribed. However, H3K27me3 enrichment of MyoD is abnormally high. This may be due to the much higher background in H3K27me3 immunoprecipitation, which is indicated by the higher H3K27me3 enrichment of negative control IGX1A than H3K4me3 enrichment. **Figure 13** shows the relative expression level of corresponding genes, which is calculated as expression level after seeding on PEGDA surfaces relative to expression level in original culture. We can see that MyoD expression level is elevated, which agrees with that MyoD gene is actively

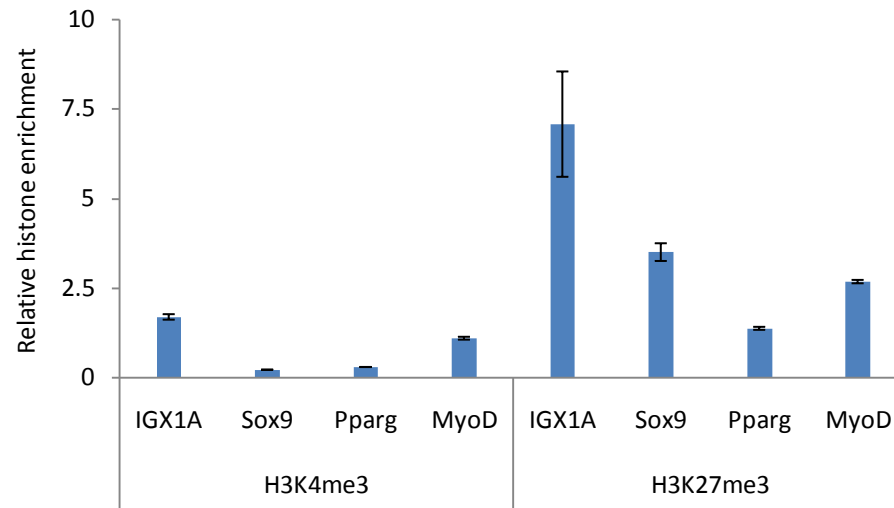


**Figure 12** Relative histone enrichment of different genes in C3H10T1/2 cells

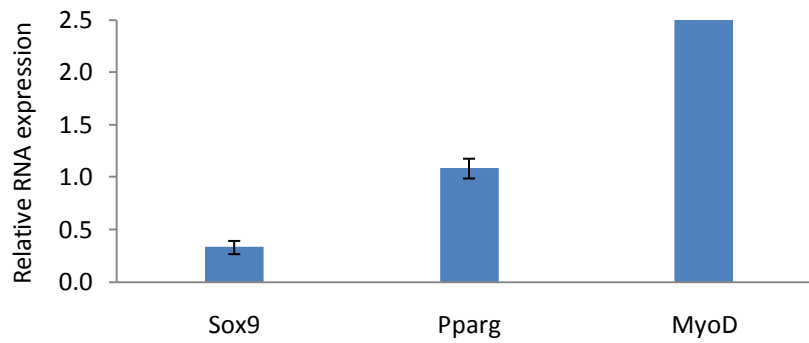


**Figure 13** Relative RNA expression level of different genes in C3H10T1/2 cells

transcribed. Moreover, from the gene expression level of cell lineage specific markers, which is controlled by its own transcription factor (Sox9, Pparg and MyoD are transcription factors for Coll2A, A-FABP and SM-22a, respectively), we found that the increased expression level of SM-22a is consistent with the increased expression level of

MyoD (**Figure 14**). ELISA result of different protein levels is somehow different from previous ChIP and gene expression profiling results (**Figure 15**). This may be caused by the unequal correlation between RNA expression level and protein expression level. And due to the high standard deviations in the assay, we can not get any statistical conclusions.

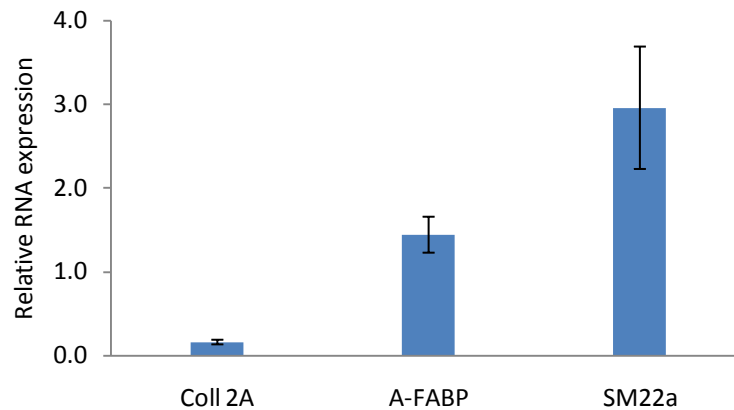


**Figure 14** Relative RNA expression level of cell markers in C3H10T1/2 cells

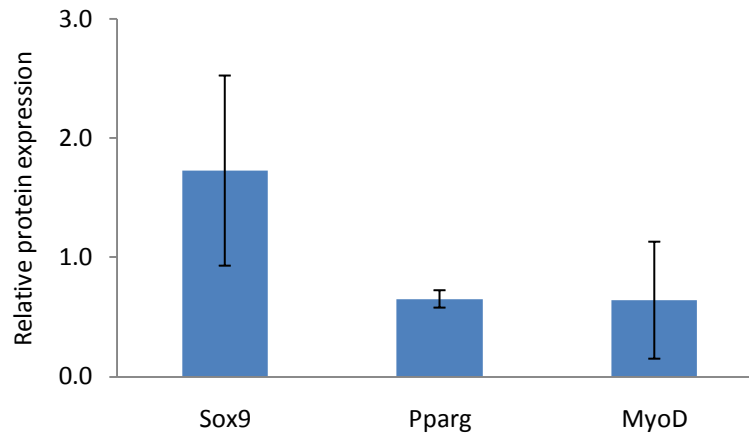


**Figure 15** Relative protein expression levels in C3H10T1/2 cells

### 2.3.3.2 NIH/3T3 model system

Similarly, **Figure 16** shows relative enrichment of transcription start sites of different genes in NIH/3T3 cells seeded on PEGDA surfaces compared to enrichment in their original culture. We can see that H3K4me3 enrichment of MyoD is greater than 1, which means MyoD gene is actively transcribed. Here, we also found that H3K27me3 enrichment of MyoD is abnormally high. This may also be resulted from the high background in H3K27me3 immunoprecipitations. **Figure 17** shows the relative expression level of corresponding genes, which is calculated as expression level after seeding on PEGDA surfaces compared to expression level in original culture. We can see that MyoD expression level is statistically elevated, which agrees with that MyoD gene is actively transcribed from chromatin state. Due to the high standard deviation in the

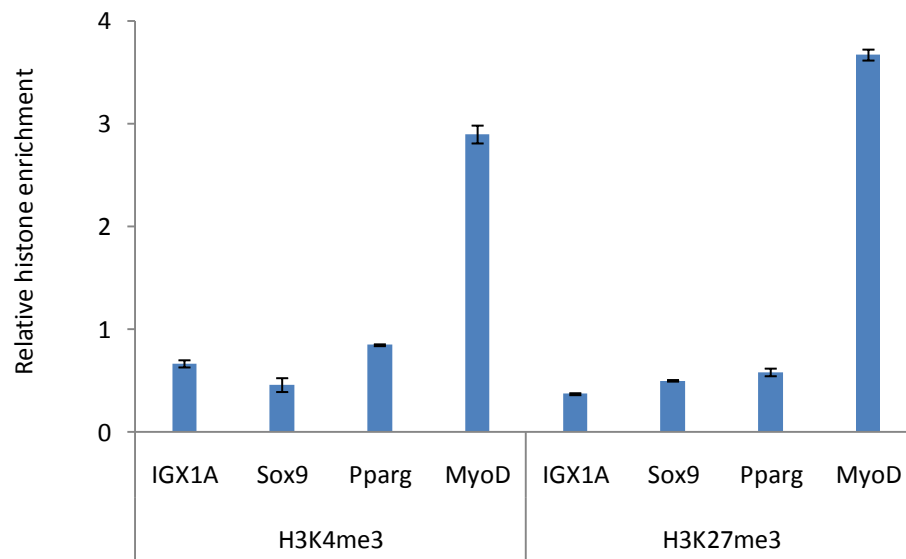


**Figure 16** Relative histone enrichment of different genes in NIH/3T3 cells

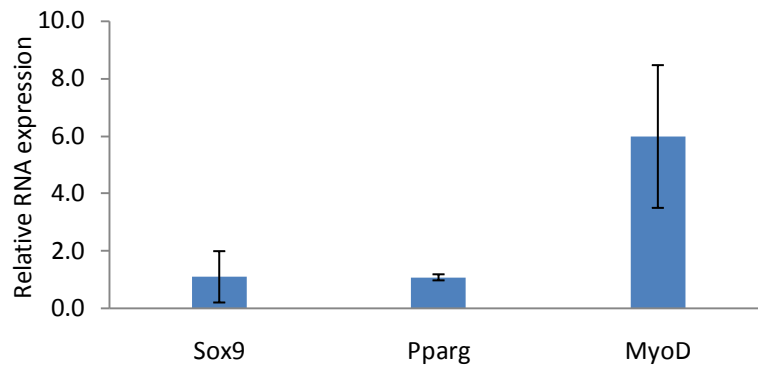


**Figure 17** Relative RNA expression level of different genes in NIH/3T3 cells

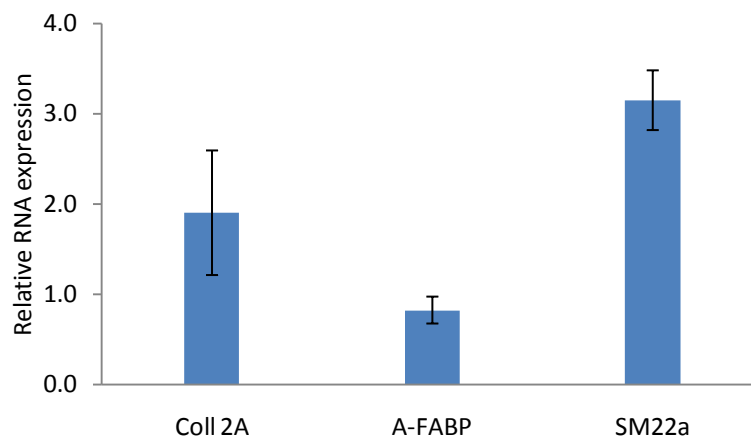


**Figure 18** Relative RNA expression level of cell markers in NIH/3T3 cells

expression level of cell lineage specific markers, we can not get any statistical conclusions about their expression. But we can still see that SM-22a expression level is qualitatively increased (**Figure 18**). ELISA result is somehow different from previous results (**Figure 19**). This may be caused by 2 reasons: 1. the high standard deviations in the assay make it impossible to get any statistical conclusions; 2. the correlation between

RNA expression level and protein expression level is unequal.

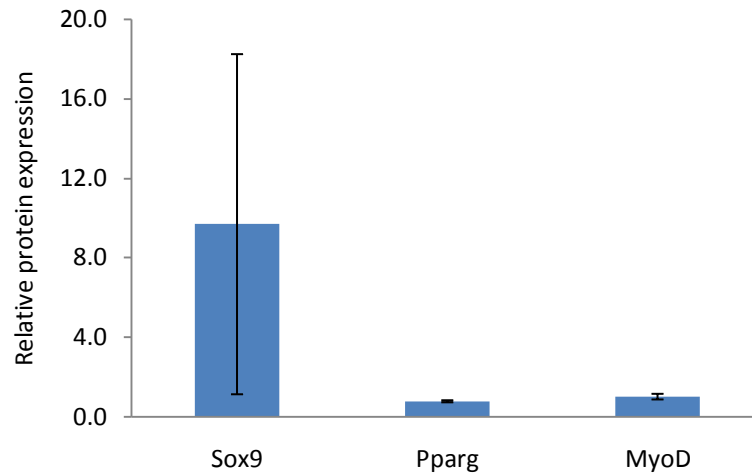


**Figure 19 Relative protein expression level in NIH/3T3 cells**

### 2.3.4 Discussion

Analysis of results above revealed that epigenetic states are changed after cells attached to matrices surfaces. As a result of the high standard deviations in the assay and the high background in H3K27me3 immunoprecipitations, we are not able to get any statistically significant conclusions.

But we can still see qualitatively that H3K4me3 enrichment of MyoD is greater than 1 in both C3H10T1/2 cells and NIH/3T3 cells, which predicts higher expression levels of myogenic markers. qRT-PCR using corresponding gene specific primers gives a similar profile predicted from epigenetic states: MyoD expression level is elevated, and SM-22a expression level is also increased, which is controlled by MyoD.

However, C3H10T1/2 cells have higher potential to be myogenic, which are determined by their origin. So this is a drawback of the study. Moreover, we can see

increased histone enrichment of other genes and increased RNA expression level of other genes. These non-specific increases may be caused by the detection limit of the methods. To get reliable results, at least  $4 \times 10^6$  cells are needed to perform 1 IP (immunoprecipitation). Due to the limit to get enough samples, we could not have so many cells for IP, which may cause the results to be a little aberrant. The non-specific increases may also be resulted from the less important role of matrix elasticity in stem cell differentiation. The modulus of PEGDA hydrogels used in the study is in the range for adipogenesis and osteogenesis, which may not be so specific for myogenesis. So other cell lineage specific genes could also have elevated expression levels.

Anyhow, from the results above, we can still see that ChIP-based epigenetic method is promising in detecting stem cell states.

### 3. CONCLUSIONS AND FUTURE DIRECTIONS

#### 3.1 Conclusions

Our data provides some preliminary perspectives on how ChIP-based epigenetic techniques can be used in tissue engineering to analyze stem cell states. After we set up the experiment system and optimized conditions, we run experiments in several model systems.

Due to the high standard deviations and the large differences in the enrichment level of negative controls in different immunoprecipitations caused by the high background in them, it is very difficult to get statistically significant conclusions. However, we can still get some qualitative conclusions about trends of different model cells.

For PEGDA matrix systems, the compression moduli of the matrix are around 40kPa, which is similar to the moduli of muscle tissues (10). Both C3H/10T1/2 and NIH/3T3 cells seeded on the matrices showed higher tendency to differentiate into muscle tissues, as is identified by higher H3K4me3 enrichment at the transcription start site of MyoD gene from chromatin state, and higher MyoD and SM-22a expression levels from RNA state. This is consistent with the prediction of cell states based on the matrices elasticity. Moreover, more transcription start sites of MyoD are bound by H3K4me3 determines the higher expression levels of MyoD and SM-22a RNA. This is consistent with the central dogma in molecular biology.

Furthermore, 3T3-L1 cells are pre-adipocytes, and upon induction, they will differentiate into mature adipocytes. The higher H3K4me3 enrichment of transcription start site of Pparg and the higher Pparg and A-FABP RNA expression levels after differentiation identify that differentiation is not fake. Although we did not check the protein expression levels of Pparg and A-FABP, we detected the morphological change and oil droplets accumulation during differentiation (data not shown).



In summary, ChIP-based epigenetic techniques are promising methods to check stem cell states. They can provide information of future cell lineages from a more fundamental level than flow cytometric profiling. If combined together with gene expression profiling or protein expression assay, more complete information can be obtained, which will help people to understand mesenchymal stem cell states and their differentiation process more clearly, more deeply and more fundamentally. This will be very beneficent for using mesenchymal stem cells in tissue engineering.

### **3.2 Future directions**

In the work above, we have shown that ChIP-based epigenetic techniques can be used to detect stem cell states for tissue engineering applications with differently modified histone enrichment at transcription start sites of different genes. Moreover, RNA profiling and protein expression level test can be used to support the conclusion obtained from epigenetic study.

We propose to build on these results in two distinct goals. First, we propose to study the effects of matrices with varying moduli on stem cell differentiation. Second, we will further study epigenetic changes in 3D cell cultures, which are more similar to cells in vivo.

#### **3.2.1 Effects of matrices elasticity on stem cell differentiation**

We can hypothesize matrices with different elasticity lead to different fates of stem cells.

In our preliminary experiments, PEGDA matrices whose moduli are in the range of muscle tissues direct stem cells to muscle-like cells. Actually, the effects of matrix elasticity on stem cell differentiation have been studied a lot (10). So we propose to investigate differently modified histone enrichment at transcription start sites of different genes specific for different cell lineages derived from the same progenitor cells.

We will use different molecular weight PEGDA to create matrices with different

moduli. Using the same procedure, we will check the epigenetic changes of stem cells seeded on matrices surfaces after culturing for 7 days compared to their states in original culture. On the other hand, Trizol-based RNA extraction will be done, which will be used in qRT-PCR to identify corresponding gene expression level. If necessary, ELISA will also be run to identify from protein expression level. We will focus on chondrogenesis specific genes, Sox9 and Col2A, adipogenesis specific genes, Pparg and A-FABP, myogenesis specific genes, MyoD and SM-22a and osteogenesis specific genes, Runx2 and Osteocalcin.

Based on our preliminary results, we can predict that H3K4me3 enrichment of transcription start site of specific gene corresponds to the cell lineage dictated by the elasticity of matrices on which stem cells are seeded. Moreover, corresponding gene expression level will also be elevated. We can also use ChIP-on-chip technique to analyze genome wide histone binding, which can give us a more complete view of the cell states.

### **3.2.2 Epigenetic changes in 3D cell cultures**

We can hypothesize 3D cell cultures are more effective in stem cell differentiation and more similar to cells in vivo.

3D cell cultures are becoming more and more important for they mimic cells in vivo (surrounded by their natural extracellular matrix), while 2D cell cultures have large differences with cells in vivo. Moreover, a lot of studies have been done in 3D cell cultures (41). So we propose to investigate epigenetic changes in 3D cell cultures.

We will encapsulate stem cells in PEGDA matrices. After culturing for 7 days, we will use microbeads to homogenize these matrices. After homogenization, cells will be released from hydrogels and then we can collect chromatin, RNA and protein samples. Then the same procedure will be done with these samples to check cell states from different levels. Then the states after encapsulating in matrices are compared with the

states in original culture to get a conclusion about differentiation.

We can predict that cells will differentiate, but we need to check very carefully which lineage they are directed to. We can use cell specific induction media to control their fates more specifically.

## REFERENCES

1. Langer, R., and Vacanti, J. P. 1994. Tissue engineering. *Science* 260: 920-926.
2. Griffith, L. G., and Naughton, G. 2002. Tissue engineering-current challenges and expanding opportunities. *Science* 295: 1009-1014.
3. Persidis, A. 1999. Tissue engineering. *Nature Biotechnology* 17: 508-510.
4. Bianco, P., and Robey, P. G. 2001. Stem cells in tissue engineering. *Nature* 414: 118-121.
5. Thomson, J. A., Itskovitz-Eldor, J., Shapiro, S. S., Waknitz, M. A., Swiergiel, J. J., Marshall, V. S., and Jones, J. M. 1998. Embryonic stem cell lines derived from human blastocysts. *Science* 282: 1145-1147.
6. Mangi, A. A., Noiseux, N., Kong, D., He, H., Rezvani, M., Ingwal, J. S., and Dzaou, V. J. 2003. Mesenchymal stem cells modified with Akt prevent remodeling and restore performance of infarcted hearts. *Nature Medicine* 9: 1195-1201.
7. Munoz-Pinto, D., Bulick, A., and Hahn M. S. 2009. Uncoupled investigation of scaffold modulus and mesh size on smooth muscle cell behavior. *J. Biomed. Mater. Res. A* 90: 303-316.
8. Liao, H., Munoz-Pinto, D., Qu, X., Hou, Y., Grunlan, M., Hahn, M. S. 2008. Influence of hydrogel mechanical properties and mesh size on vocal fold fibroblast extracellular matrix production. *Acta Biomaterialia* 4: 1161-1171.
9. Mastitskaya, S., and Denecke, B. 2009. Human spongiosa mesenchymal stem cells fail to generate cardiomyocytes *in vitro*. *Journal of Negative Results in BioMedicine* 8:11-24.
10. Engler, A. J., Sen, S., Sweeney, H. L., and Discher, D. E. 2006. Matrix elasticity directs stem cell lineage specification. *Cell* 126: 677-689.

11. Giancotti, F. G., and Ruoslahti, E. 1999. Integrin signaling. *Science* 285: 1028-1032.
12. Connelly, J. T., Garcia, A. J., and Levenston, M.E. 2007. Inhibition of in vitro chondrogenesis in RGD-modified three-dimensional alginate gels. *Biomaterials* 28: 1071–1083.
13. Terraciano, V., Hwang, N., Moronl, L., Park, H. B., Zhang, Z., Mizrahi, J., Seliktar, D., and Elisseeff, J. 2007. Differential response of adult and embryonic mesenchymal progenitor cells to mechanical compression in hydrogels. *Stem Cells* 25: 2730-2738.
14. Javazon, E. H., Beggs, K. J., and Flake, A. W. 2004. Mesenchymal stem cells: paradoxes of passaging. *Experimental Hematology* 32: 414–425.
15. Koike, N., Fukumura, D., Gralla, O., Au, P., Schechner, J. S., and Jain, R. K. 2004. Creation of long-lasting blood vessels. *Nature* 428: 138-139.
16. Viravaidya, K., and Shuler, M. L. 2004. Incorporation of 3T3-L1 cells to mimic bioaccumulation in a microscale cell culture analog device for toxicity studies. *Biotechnol. Prog.* 20: 590-597.
17. Salem, A. K., Stevens, R., Pearson, R. G., Davies, M. C., Tendler, S. J. B., Roberts, C. J., Williams, P. M., and Shakesheff, K. M. 2002. Interactions of 3T3 fibroblasts and endothelial cells with defined pore features. *Tissue Engineering. Part A* 15: 1053-1061.
18. Russo, V. E. A., Martienssen, R. A., Riggs, A. D. 1996. *Epigenetic Mechanisms of Gene Regulation*. (Cold Spring Harbor Laboratory Press, NY)
19. Reik, W., Dean, W., Walter, J. 2001. Epigenetic reprogramming in mammalian development. *Science* 293: 1089-1093.
20. Guenther, M. G., Levine, S. L., Boyer, L. A., Jaenisch, R., and Young, R. A. 2007. A chromatin landmark and transcription initiation at most promoters in human cells. *Cell* 130: 77-88.

21. Benoit, D. S. W., Schwartz, M. P., Durney, A. R., and Anseth, K. S. 2008. Small functional groups for controlled differentiation of hydrogel-encapsulated human mesenchymal stem cells. *Nature Materials* 7: 816-823.
22. Huebsch, N., Arany, P. R., Mao, A. S., Shvartsman, D., Ali, O. A., Bencherif, S. A., Rivera-Feliciano, J and Mooney, D. J. 2010. Harnessing traction-mediated manipulation of the cell/matrix interface to control stem-cell fate. *Nature Materials* 9: 518-526.
23. Phelps, E. A., Landazuri, N., Thule, P. M., Taylor, W. R., and Garcia, A. J. 2009. Bioartificial matrices for therapeutic vascularization. *Proc. Natl. Acad. Sci. USA* 107: 3323-3328.
24. Lutolf, M. P., Lauer-Fields, J. L., Schmoekel, H. G., Metters, A. T., Weber, F. E., Fields, G. B., and Hubbell, J. A. 2003. Synthetic matrix metalloproteinase-sensitive hydrogels for the conduction of tissue regeneration: Engineering cell-invasion characteristics. *Proc. Natl. Acad. Sci. USA* 100:5413–5418.
25. Sato, N., Sanjuan, I. M., Heke, M., Uchida, M., Naef, F., and Brivanlou, A. H. 2003. Molecular signature of human embryonic stem cells and its comparison with the mouse. *Dev. Biol.* 260: 404–413.
26. Jiang, Y., Jahagirdar, B. N., Reinhardt, R. L., Schwartz, R. E., Keene, C. D., Ortiz-Gonzalez, X. R., Reyes, M., Lenvik, T., Lund, T., Blackstad, M., Du, J., Aldrich, S., Lisberg, A., Low, W. C., Largaespada, D. A., and Verfaillie, C. M. 2002. Pluripotency of mesenchymal stem cells derived from adult marrow. *Nature* 418: 41-49.
27. Ohlsson, R., and Kanduri, C. 2002. New twists on the epigenetics of CpG islands. *Genome Res.* 12: 525-526.
28. Vaissiere, T., Sawan, C., Herceg, Z. 2008. Epigenetic interplay between histone modifications and DNA methylation in gene silencing. *Mutation Research* 659: 40–48.
29. Jenuwein, T., and Allis, C. D. 2001. Translating the histone code. *Science* 293: 1074-1080.

30. Lachner, M., O'Sullivan, R. J., and Jenuwein, T. 2003. An epigenetic road map for histone lysine methylation. *Journal of Cell Science* 116: 2117-2124.
31. Bannister, A. J., and Kouzarides, T. 2005. Reversing histone methylation. *Nature* 436: 1103-1106.
32. Strahl, B. D., and Allis, C. D. 2000. The language of covalent histone modifications. *Nature* 403: 41-45.
33. Bernstein, B. E., Kamal, M., Lindblad-Toh, K., Bekiranov, S., Bailey, D. K., Huebert, D. J., McMahon, S., Karlsson, E. K., Kulbokas, E. J. III, Gingeras, T. R., Schreiber, S. L., and Lander, E. S. 2005. Genomic maps and comparative analysis of histone modifications in human and mouse. *Cell* 120: 169-181.
34. Wells, J., and Farnham, P. J. 2002. Characterizing transcription factor binding sites using formaldehyde crosslinking and immunoprecipitation. *Methods* 1:48-56.
35. Collas, P. 2010. The current state of chromatin immunoprecipitation. *Mol. Biotechnol.* 45:87-100.
36. Harris, J. M. 1992. Poly (ethylene glycol) Chemistry: Biotechnical and Biomedical Applications. (Plenum Press, New York)
37. Park, J. S., Chu, J. S. F., Cheng, C., Chen, F., Chen, D., Li, S. 2004. Differential effects of equiaxial and uniaxial strain on mesenchymal stem cells. *Biotechnology and Bioengineering* 88: 359-368.
38. Madsen, L., Petersen, R. K., Sorensen, M. B., Jorgensen, C., Hallenborg, P., Pridal, L., Fleckner, J., Amri, E., Krieg, P., Furstenberger, G., Berge, R. K., and Kristiansen, K. 2003. Adipocyte differentiation of 3T3-L1 preadipocytes is dependent on lipoxygenase activity during the initial stages of the differentiation process. *Biochem. J.* 375: 539-549.
39. Kim, B. S., and Mooney, D. J. 1998. Development of biocompatible synthetic extracellular matrices for tissue engineering. *Trends in Biotechnology* 16: 224-230.
40. Ruoslahti, E., and Pierschbacher, M. D. 1987. New perspectives in cell adhesion: RGD and integrins. *Science* 238: 491-497.

41. Tibbitt, M. A., and Anseth, K. S. 2009. Hydrogels as extracellular matrix mimics for 3D cell culture. *Biotechnology and Bioengineering* 103: 655-663.



**VITA**

Name: Bo Wang

Address: Artie McFerrin Department of Chemical Engineering, Texas A&M University, Jack E. Brown Engineering Building, 3122 TAMU, Room 200, College Station, TX 77843-3122

Email Address: wangbo-tju@neo.tamu.edu

Education: B.S., Biological Engineering, Tianjin University, 2008